arXiv:1302.2301v1 [nucl-th] 10 Feb 2013

Signature of strange dibaryons in kaon- and photon-induced reactions

Shota Ohnishi,[1,2,*] Yoichi Ikeda,[2] Hiroyuki Kamano,[3] and Toru Sato[4,5]

[1] *Department of Physics, Tokyo Institute of Technology, Tokyo 152-8551, Japan*

[2] *RIKEN Nishina Center, Wako, Saitama 351-0198, Japan*

[3] *Research Center for Nuclear Physics,*
Osaka University, Osaka 567-0047, Japan

[4] *Department of Physics, Osaka University, Osaka 560-0043, Japan*

[5] *J-PARC Branch, KEK Theory Center,*
Institute of Particle and Nuclear Studies, KEK,
203-1, Shirakata, Tokai, Ibaraki, 319-1106, Japan

(Dated: February 12, 2013)

Abstract

We examine how the signature of the strange dibaryon resonances shows up in scattering amplitudes and observables of the three-body $\bar{K}NN$-πYN ($Y=\Sigma,\ \Lambda$) system on the physical real energy axis. The so-called point method is applied to handle logarithmic singularities that appear in solving the Alt-Grassberger-Sandhas equations for the real scattering energies. By taking two different kinds of models for the two-body $\bar{K}N$-$\pi\Sigma$ subsystem, both of which reproduce the available data equally well but give quite a different resonance-pole structure for $\Lambda(1405)$, we also investigate whether the strange-dibaryon production reactions can be used for disentangling the nature of $\Lambda(1405)$.

---

[*] Electronic address: s˙ohnishi@riken.jp

I. INTRODUCTION

In recent years, the strange dibaryons have been studied actively as the simplest kaonic nuclei [1] in the three-body $\bar{K}NN$-πYN system. A number of theoretical studies to search for the strange dibaryons have been performed with the variational method [2–5] and the Alt-Grassberger-Sandhas (AGS) equations [6–8], employing the phenomenological potentials [2, 4, 6] or the effective chiral Lagrangian [3, 5, 7–9] for the meson-baryon and baryon-baryon interactions. All the studies support the existence of the strange dibaryons as resonance states in the energy region between the $\bar{K}NN$ and $\pi\Sigma N$ thresholds. However, the resonance energies predicted in those studies are still highly model-dependent. For example, the models with energy independent potentials [2, 4, 6, 7] give the resonance energies lower than those with energy dependent potentials [3, 5, 8].

In parallel with the theoretical works mentioned above, experimental searches for the strange dibaryons have also been done by the FINUDA Collaboration [10], the OBELIX Collaboration [11], and the DISTO Collaboration [12]. Further data will become available from SPring-8 (LEPS Collaboration [13]) and GSI (FOPI Collaboration [14]), and new experiments are planned at J-PARC (E15 [15] and E27 [16] experiments) and DAΦNE (AMADEUS Collaboration [17]).

In our previous works [7, 8], we have investigated a possible existence of the strange dibaryon resonances in the three-body $\bar{K}NN$-$\pi\Sigma N$ system. This has been achieved by searching for resonance poles of the three-body amplitudes in the complex energy plane, where the amplitudes are obtained by solving the coupled-channel AGS equations. There, two models, the energy-independent (E-indep) and the energy-dependent (E-dep) models, have been employed for the s-wave meson-baryon interactions, both of which are derived from the leading-order term of the effective chiral Lagrangian but those have different off-shell behavior. As a result, we have found one resonance pole of the strange dibaryon for the E-indep model while two for the E-dep model, which is summarized in Table I. This result indicates that off-shell behavior of the meson-baryon interactions of the two-body $\bar{K}N$-πY subsystem is crucial for the resulting pole positions of the strange dibaryon resonances.

Most of the theoretical studies have presented just pole positions of the strange dibaryon resonances. However, those are not a quantity that can be directly measured in experiments. In order to examine the existence of the strange dibaryons in connection with experiments,

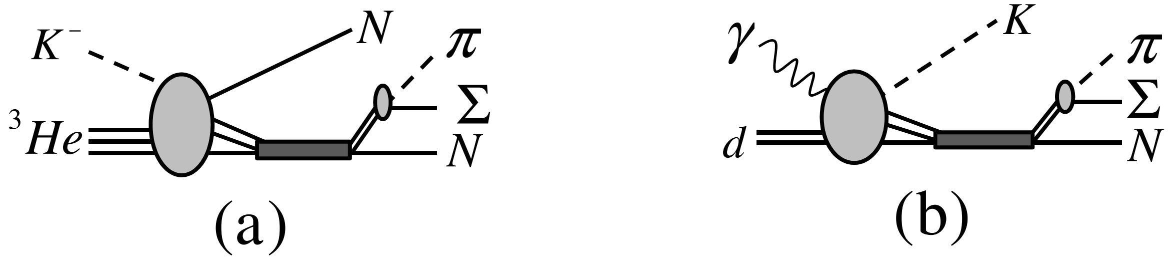

FIG. 1: Examples of the typical (a)kaon- and (b)photon-induced strange dibaryon production reactions. The strange dibaryon resonances would be produced in thick shaded boxes.

TABLE I: Pole masses M_R of the strange dibaryon resonances obtained in our previous works [7, 8]. See the text for the explanation on the E-indep and E-dep models.

	$\mathrm{Re}(M_R)$ (MeV)	$-\mathrm{Im}(M_R)$ (MeV)
E-indep model	2312-2326	17-20
E-dep model	2354-2361	17-23
	2281-2303	122-160

one has to compute the cross sections of strange-dibaryon production reactions consistently in the same framework. The strange dibaryon resonances can be produced via, for example, kaon- and photon-induced reactions on light nuclei such as ^{3}He and deuteron (Fig. 1). Then the signal of the resonances would be observed in the invariant-mass and/or missing-mass distributions of the decay products. A couple of such studies have been performed by Koike-Harada [18] and Yamagata *et al.* [19] on the basis of the optical potential approach.

In this work, we examine how the signature of the strange dibaryons shows up in the observables of the three-body reactions by applying our approach based on the coupled-channel AGS equations developed in Refs. [7, 8]. It is well known that logarithmic singularities appear when one solves the AGS equations for the break-up reactions at real scattering energies. We handle those singularities numerically by making use of the so-called point-method proposed by Schlessinger [22] and developed by Kamada *et al.* [23]. With this method, we examine the behavior of the quasi-two-body amplitudes (the thick shaded boxes in Fig. 1) of the $\bar{K}NN$-πYN system at real scattering energies between the $\bar{K}NN$ and $\pi\Sigma N$ thresholds. Also, as a first step toward developing a model to compute reaction cross sections measured at the facilities such as J-PARC and SPring-8 (e.g., the reactions in Fig. 1), we examine the "transition probability" of a strange-dibaryon production reaction, $(Y_K)_{I=0}+N \to \pi+\Sigma+N$, where $(Y_K)_{I=0}$ is an "isobar" of $\bar{K}N$ states with isospin $I=0$.

In Sec. II, we explain the AGS equations for the three-body $\bar{K}NN$-$\pi YN(Y=\Sigma,\Lambda)$ system and present the transition probability formula for break-up reactions. Then, we present the two-body meson-baryon interactions used in this work in Sec. III. The computed quasi-two-body amplitudes as well as transition probabilities for $(Y_K)_{I=0}+N \to \pi+\Sigma+N$ are presented in Sec. IV. Summary is given in Sec. V. A brief description of the point method is presented in Appendix.

II. THREE-BODY EQUATIONS

A. Alt-Grassberger-Sandhas equations

Throughout this paper, we assume that the three-body processes take place via separable two-body interactions, which have the following form in the two-body center-of-mass (CM) frame,

$$V_{(\alpha)_I i,(\beta)_I i}(\vec{q}_i{}', \vec{q}_i; E) = g^*_{(\alpha)_I}(\vec{q}_i{}')\lambda_{(\alpha)_I i,(\beta)_I i}(E) g_{(\beta)_I}(\vec{q}_i) \ , \tag{1}$$

where $g_{(\alpha)_I}(\vec{q}_i)$ is the cutoff factor of the two-body channel $\alpha(=jk)$ with a relative momentum $\vec{q}_i$ and isospin I; E is the total energy of the two-body system. In the three-body system, we define the two-body energy E as $E = W - E_i(\vec{p}_i)$ with three-body energy W and the spectator particle energy $E_i(\vec{p}_i)$, where $\vec{p}_i$ is the relative momentum of the spectator particle i. The explicit forms of each two-body interaction are presented in detail in Sec. III.

The assumption above implies that two-body subsystems in the three-body processes form an "isobar" and thus the processes can be described as a quasi-two-body scattering of the isobar and the spectator particle. The quasi-two-body amplitudes, $X_{(\alpha)_I i,(\beta)_{I'} j}(\vec{p}_i, \vec{p}_j; W)$, are then obtained by solving the AGS equations [20, 21],

$$\begin{aligned} X_{(\alpha)_I i,(\beta)_{I'} j}(\vec{p}_i, \vec{p}_j, W) &= (1-\delta_{ij}) Z_{(\alpha)_I i,(\beta)_{I'} j}(\vec{p}_i, \vec{p}_j, W) \\ &\quad + \sum_{(\gamma),(\delta)} \sum_{I''} \sum_{n \neq i} \int d\vec{p}_n Z_{(\alpha)_I i,(\gamma)_{I''} n}(\vec{p}_i, \vec{p}_n, W) \\ &\quad \times \tau_{(\gamma)_{I''} n,(\delta)_{I''} n}\left(W - E_n(\vec{p}_n), \vec{p}_n\right) X_{(\delta)_{I''} n,(\beta)_{I'} j}(\vec{p}_n, \vec{p}_j, W) \ . \end{aligned} \tag{2}$$

TABLE II: Indices specifying the “isobars”.

Isobar	Allowed isospin(s)	Spectator particle	three-body Fock space
$(Y_K) = (\bar{K}N_2), (\bar{K}N_1)$	0, 1	N_1, N_2	$\left\lvert N_1 N_2 \bar{K} \right\rangle$
$(Y_\pi) = (\pi\Sigma)$	0, 1	N	$\lvert N\Sigma\pi\rangle, \lvert \Sigma N\pi\rangle$
$(Y_\pi) = (\pi\Lambda)$	1	N	$\lvert N\Lambda\pi\rangle, \lvert \Lambda N\pi\rangle$
$(d) = (NN)$	1	$\bar{K}$	$\left\lvert N_1 N_2 \bar{K} \right\rangle$
$(N^*) = (\pi N)$	1/2, 3/2	Σ	$\lvert \Sigma N\pi\rangle, \lvert N\Sigma\pi\rangle$
$(N^*) = (\pi N)$	1/2	Λ	$\lvert \Lambda N\pi\rangle, \lvert N\Lambda\pi\rangle$
$(d_y) = (\Sigma N)$	1/2, 3/2	π	$\lvert \Sigma N\pi\rangle, \lvert N\Sigma\pi\rangle$
$(d_y) = (\Lambda N)$	1/2	π	$\lvert \Lambda N\pi\rangle, \lvert N\Lambda\pi\rangle$

Here, $(\alpha)_I$ denotes the isobar formed by a two-particle pair α with isospin I; the subscripts i, j, n represent the spectator particles. The notations for the isobars are summarized in Table II.

The driving term $Z_{(\alpha)_I i,(\beta)_{I'} j}(\vec{p}_i, \vec{p}_j; W)$ describes a particle-exchange potential given by [see Fig. 2 (a) for the kinematics]

$$Z_{(\alpha)_I i,(\beta)_{I'} j}(\vec{p}_i, \vec{p}_j; W) = \frac{g_{(\alpha)_I}(\vec{q}_i) g^*_{(\beta)_{I'}}(\vec{q}_j)}{W - E_i(\vec{p}_i) - E_j(\vec{p}_j) - E_k(\vec{p}_k) + i\epsilon}, \tag{3}$$

where $E_i(\vec{p}_i)$ and $E_j(\vec{p}_j)$ are the energies of the spectator particles i and j, respectively; $E_k(\vec{p}_k)$ with $\vec{p}_k = -\vec{p}_i - \vec{p}_j$ is the energy of the exchange particle k; $\vec{q}_i$ ($\vec{q}_j$) is the relative momentum between the exchange-particle and the spectator-particle j (i). In the nonrelativistic kinematics, we have $E_n(\vec{p}_n) = m_n + \vec{p}_n^2/(2m_n)$ ($n = i, j, k$) and $\vec{q}_{i,j} = (m_{k,i}\vec{p}_{j,k} - m_{j,k}\vec{p}_{k,i})/(m_{j,k} + m_{k,i})$. The s-wave projection of $Z_{(\alpha)_I i,(\beta)_{I'} j}(\vec{p}_i, \vec{p}_j; W)$ is given by

$$Z_{(\alpha)_I i,(\beta)_{I'} j}(p_i, p_j; W) = \frac{1}{2}\int_{-1}^{1} d(\cos\theta) Z_{(\alpha)_I i,(\beta)_{I'} j}(\vec{p}_i, \vec{p}_j; W), \tag{4}$$

with $\cos\theta = \hat{p}_i \cdot \hat{p}_j$.

The isobar propagator, $\tau_{(\alpha)_I i,(\beta)_I i}(W - E_i(\vec{p}_i), \vec{p}_i)$ as illustrated in Fig. 2 (b), is given in

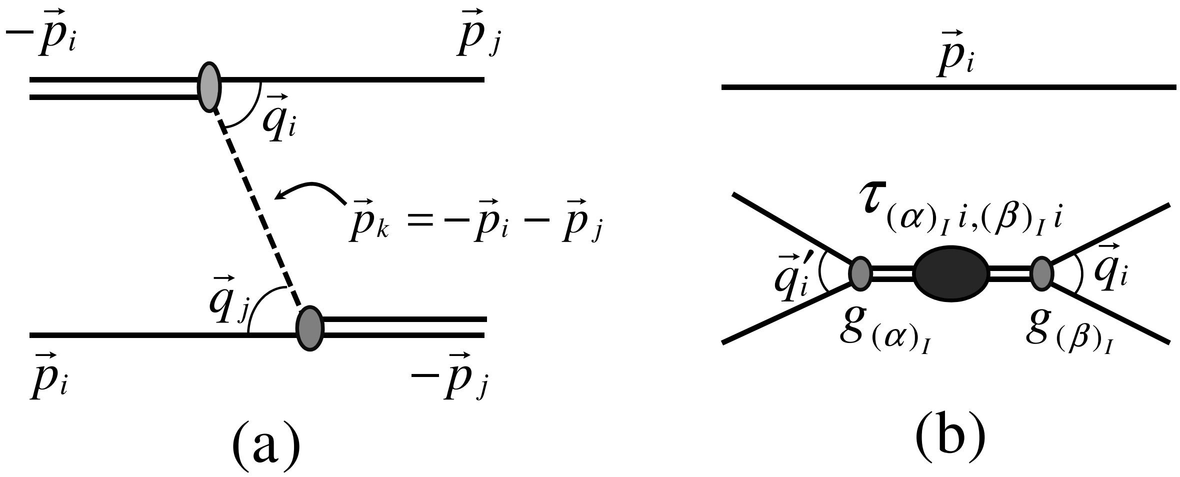

FIG. 2: (a) One particle exchange interaction $Z_{(\alpha)_I i,(\beta)_{I'} j}(p_i, p_j, W)$. (b) Isobar propagator $\tau_{(\alpha)_I i,(\beta)_I i}(W - E_i(\vec{p}_i), \vec{p}_i)$.

the nonrelativistic kinematics by solving the following Lippmann-Schwinger equations,

$$\tau_{(\alpha)_I i,(\beta)_I i}(W - E_i(\vec{p}_i), \vec{p}_i) = \lambda_{(\alpha)_I i,(\beta)_I i} + \sum_{(\gamma)} \int q_i^2 dq_i \frac{\lambda_{(\alpha)_I i,(\gamma)_I i} |g_{(\gamma)_I}(q_i)|^2}{W - E_i(\vec{p}_i) - E_{jk}(\vec{p}_i, \vec{q}_i)} \tau_{(\gamma)_I i,(\beta)_I i}(W - E_i(\vec{p}_i), \vec{p}_i) \quad . \tag{5}$$

Here, $E_{jk}(\vec{p}_i, \vec{q}_i)$ is the energy of the interacting pair (jk), $E_{jk}(\vec{p}_i, \vec{q}_i) = m_j + m_k + \vec{p}_i^2/2(m_j + m_k) + \vec{q}_i^2/2\mu_i$ with the reduced mass defined as $\mu_i = m_j m_k/(m_j + m_k)$.

After taking antisymmetrization for the two-nucleon states in the three-body processes, the AGS equations (2) are formally written as (suppressing all indices other than that of the isobars)

$$
\begin{pmatrix} X_{(Y_K),(Y_K)} \\ X_{(Y_\pi),(Y_K)} \\ X_{(d),(Y_K)} \\ X_{(N^*),(Y_K)} \\ X_{(d_y),(Y_K)} \end{pmatrix}
=
\begin{pmatrix} Z_{(Y_K),(Y_K)} \\ 0 \\ Z_{(d),(Y_K)} \\ 0 \\ 0 \end{pmatrix}
$$

$$
-\begin{pmatrix}
Z_{(Y_K),(Y_K)}\tau_{(Y_K),(Y_K)} & Z_{(Y_K),(Y_K)}\tau_{(Y_K),(Y_\pi)} & 2Z_{(Y_K),(d)}\tau_{(d),(d)} & 0 & 0 \\
0 & 0 & 0 & Z_{(Y_\pi),(N^*)}\tau_{(N^*),(N^*)} & Z_{(Y_\pi),(d_y)}\tau_{(d_y),(d_y)} \\
Z_{(d),(Y_K)}\tau_{(Y_K),(Y_K)} & Z_{(d),(Y_K)}\tau_{(Y_K),(Y_\pi)} & 0 & 0 & 0 \\
Z_{(N^*),(Y_\pi)}\tau_{(Y_\pi),(Y_K)} & Z_{(N^*),(Y_\pi)}\tau_{(Y_\pi),(Y_\pi)} & 0 & 0 & Z_{(N^*),(d_y)}\tau_{(d_y),(d_y)} \\
Z_{(d_y),(Y_\pi)}\tau_{(Y_\pi),(Y_K)} & Z_{(d_y),(Y_\pi)}\tau_{(Y_\pi),(Y_\pi)} & 0 & Z_{(d_y),(N^*)}\tau_{(N^*),(N^*)} & 0
\end{pmatrix}
$$

$$
\times \begin{pmatrix} X_{(Y_K),(Y_K)} \\ X_{(Y_\pi),(Y_K)} \\ X_{(d),(Y_K)} \\ X_{(N^*),(Y_K)} \\ X_{(d_y),(Y_K)} \end{pmatrix}. \tag{6}
$$

B. Break-up reactions

In this subsection, we present formulas for computing transition probability of the quasi-2-body to 3-body reaction, $(Y_K)_{I=0} + N \to \pi + \Sigma + N$. For this purpose, we first need to define the amplitudes of the $(Y_K)_{I=0} + N \to \pi + \Sigma + N$ reaction. This is because within our formulation the well-defined amplitudes are of the 3-body to 3-body scatterings, where all the external particles are stable against strong interactions. The relevant amplitude here is of the $(\bar{K} + N) + N \to (Y_K)_{I=0} + N \to \pi + \Sigma + N$ reaction, which is given in a concise notation as

$$
T_{\pi\Sigma N \leftarrow (\bar{K}N)N} = \sum_{(\alpha)i=\pi\Sigma N} \sum_{(\gamma)} \sum_{I} g^*_{(\alpha)_I} \tau_{(\alpha)_I i,(\gamma)_I i} X_{(\gamma)_I i,(Y_K)_{I=0}N} \tau_{(Y_K)_{I=0}N,(Y_K)_{I=0}N} g_{(Y_K)_{I=0}}, \tag{7}
$$

where the summation of $(\alpha)i$ is taken for all possible combinations of $\pi\Sigma N$. Now let us consider the isobar $(Y_K)_{I=0}$ as an actual resonance state of the two-body reactions. (Note that we originally introduced notion of the isobars just for the sake of convenience in our formulation and did not take them as actual resonances.) Near a resonance pole of the isobar propagator $\tau_{(Y_K)_{I=0},(Y_K)_{I=0}}(E)$, the two-body amplitude for $\bar{K}N_{I=0} \to \bar{K}N_{I=0}$ can be approximated as

$$\begin{aligned} t_{(Y_K)_{I=0},(Y_K)_{I=0}}(E) &= g^*_{(Y_K)_{I=0}} \tau_{(Y_K)_{I=0},(Y_K)_{I=0}}(E,\vec{0}) g_{(Y_K)_{I=0}} \\ &\sim g^*_{(Y_K)_{I=0}} \frac{\sqrt{R_{(Y_K)_{I=0}}}\sqrt{R_{(Y_K)_{I=0}}}}{E - M + i\Gamma/2} g_{(Y_K)_{I=0}} \\ &\equiv \bar{g}^*_{\bar{K}N\leftarrow Y_K} \frac{1}{E - M + i\Gamma/2} \bar{g}_{Y_K \leftarrow \bar{K}N}, \end{aligned} \tag{8}$$

where $M - i\Gamma/2$ is the resonance pole position of $\tau_{(Y_K)_{I=0},(Y_K)_{I=0}}(E)$ and $R_{(Y_K)_{I=0}}$ is the residue of $\tau_{(Y_K)_{I=0},(Y_K)_{I=0}}$ at the pole. Also, $\bar{g}_{Y_K\leftarrow\bar{K}N} = \sqrt{R_{(Y_K)_{I=0}}} g_{(Y_K)_{I=0}}$ $[\bar{g}_{\bar{K}N\leftarrow Y_K} = \sqrt{R_{(Y_K)_{I=0}}} g^*_{(Y_K)_{I=0}}]$ can be interpreted as a vertex function for the process $\bar{K}N_{I=0} \to (Y_K)_{I=0}$ $[(Y_K)_{I=0} \to \bar{K}N_{I=0}]$. Within this approximation, the three-body amplitude can be written as

$$\begin{aligned} T_{\pi\Sigma N\leftarrow(\bar{K}N)N} &= \sum_{(\alpha)i=\pi\Sigma N} \sum_{(\gamma)} \sum_{I} g^*_{(\alpha)_I} \tau_{(\alpha)_I i,(\gamma)_I i} X_{(\gamma)_I i,(Y_K)_{I=0}N} \\ &\times\ \tau_{(Y_K)_{I=0}N,(Y_K)_{I=0}N}(W - E_N(\vec{p}_N), \vec{p}_N) g_{(Y_K)_{I=0}} \\ &\sim \sum_{(\alpha)i=\pi\Sigma N} \sum_{(\gamma)} \sum_{I} g^*_{(\alpha)_I} \tau_{(\alpha)_I i,(\gamma)i} X_{(\gamma)i,(Y_K)_{I=0}N} \\ &\times\ \sqrt{R_{(Y_K)_{I=0}}} G_{(Y_K)_{I=0}}(W - E_N(\vec{p}_N), \vec{p}_N) \bar{g}_{Y_K\leftarrow\bar{K}N}, \end{aligned} \tag{9}$$

where $G_{(Y_K)_{I=0}}(W - E_N(\vec{p}_N), \vec{p}_N)$ is the $(Y_K)_{I=0}$ resonance propagator in the existence of a spectator nucleon with momentum $\vec{p}_N$. From Eq. (9), it is reasonable to define T-matrix of $(Y_K)_{I=0} + N \to \pi + \Sigma + N$ as

$$T_{\pi\Sigma N\leftarrow(Y_K)_{I=0}N} = \sum_{(\alpha)i=\pi\Sigma N} \sum_{(\gamma)} \sum_{I} g^*_{(\alpha)_I} \tau_{(\alpha)_I i,(\gamma)_I i} X_{(\gamma)_I i,(Y_K)_{I=0}N} \sqrt{R_{(Y_K)_{I=0}}}. \tag{10}$$

The s-wave projection of the scattering amplitudes for the $(Y_K)_{I=0} + N \to \pi + \Sigma + N$

reaction are then given by

$$
\begin{aligned}
&T_{\pi\Sigma N\text{-}(Y_K)_{I=0}N}(\vec{q}_N,\vec{p}_N,p'_N,W)\\
&=(4\pi)^{-3/2}\sum_I\\
&\times\{\left|[[\pi\otimes\Sigma]_{(Y_\pi)_I}\otimes N]_\Gamma\right\rangle g_{(Y_\pi)_I}(q_N)\tau_{(Y_\pi)_I N,(Y_K)_I N}\left(W-E_N(\vec{p}_N)\right)X_{(Y_K)_I N,(Y_K)_{I=0}N}(p_N,p'_N,W)\\
&+\left|[[\pi\otimes\Sigma]_{(Y_\pi)_I}\otimes N]_\Gamma\right\rangle g_{(Y_\pi)_I}(q_N)\tau_{(Y_\pi)_I N,(Y_\pi)_I N}\left(W-E_N(\vec{p}_N)\right)X_{(Y_\pi)_I N,(Y_K)_{I=0}N}(p_N,p'_N,W)\\
&+\left|[[\pi\otimes N]_{(N^*)_I}\otimes\Sigma]_\Gamma\right\rangle g_{(N^*)_I}(q_\Sigma)\tau_{(N^*)_I\Sigma,(N^*)_I\Sigma}\left(W-E_\Sigma(\vec{p}_\Sigma)\right)X_{(N^*)_I\bar{K},(Y_K)_{I=0}N}(p_\Sigma,p'_N,W)\\
&+\left|[[\Sigma\otimes N]_{(d_y)_I}\otimes\pi]_\Gamma\right\rangle g_{(d_y)_I}(q_\pi)\tau_{(d_y)_I\pi,(d_y)_I\pi}\left(W-E_\pi(\vec{p}_\pi)\right)X_{(d_y)_I\pi,(Y_K)_{I=0}N}(p_\pi,p'_N,W)\}\\
&\times\langle[(Y_K)_{I=0}\otimes N']_{\Gamma'}|\sqrt{R_{(Y_K)_{I=0}}}\ ,
\end{aligned}
\tag{11}
$$

where $|[A\otimes B]_a\otimes C]_b\rangle$ with $(ABC)=(\pi\Sigma N)$ and $|[(Y_K)_{I=0}\otimes N]_b\rangle$ are the spin-isospin wave functions of the final and initial states, and $X_{(\alpha)_I i,(\beta)_{I'}j}(p,p',W)$ is the s-wave projection of the quasi-two-body amplitudes given in Eqs. (2) and (6). The momentum q_Σ, q_π, p_Σ and p_π are function of $\vec{q}_N$ and $\vec{p}_N$, i.e., $q_\Sigma(\vec{q}_N,\vec{p}_N)$, $q_\pi(\vec{q}_N,\vec{p}_N)$, $p_\Sigma(\vec{q}_N,\vec{p}_N)$ and $p_\pi(\vec{q}_N,\vec{p}_N)$.

Using Eq. (11), we define the transition probability of $(Y_K)_{I=0}+N\to\pi+\Sigma+N$ as follows,

$$
w(p'_N,W)=2\pi\int d^3\vec{p}_N d^3\vec{q}_N\sum_{f\bar{i}}\delta\left(W-M-\frac{\vec{p}_N^2}{2\eta_N}-\frac{\vec{q}_N^2}{2\mu_N}\right)\left|T_{\pi\Sigma N-(Y_K)_{I=0}N}\left(\vec{q}_N,\vec{p}_N,p'_N,W\right)\right|^2\ .
\tag{12}
$$

III. MODEL OF TWO-BODY INTERACTIONS

Now we present explicit forms of the two-body interactions [Eq. (1)] used in this work. We first consider the meson-baryon interactions (Sec. III A), and then consider the baryon-baryon interactions (Sec. III B). In this section, we suppress indices of the spectator.

A. Meson-baryon interaction

As done in our earlier works [7, 8], we consider two kinds of models for the s-wave meson-baryon interactions, which are called the E-indep and E-dep models, respectively. The explicit forms are given by

$$
V^{\text{E-indep}}_{(\alpha)_I(\beta)_I}(q',q)=-C_{(\alpha)_I(\beta)_I}\frac{1}{32\pi^2F_\pi^2}\frac{m_\alpha+m_\beta}{\sqrt{m_\alpha m_\beta}}g_{(\alpha)_I}(q')g_{(\beta)_I}(q),
\tag{13}
$$

for the E-indep model, and by

$$V^{\text{E-dep}}_{(\alpha)_I(\beta)_I}(q',q;E) = -C_{(\alpha)_I(\beta)_I}\frac{1}{32\pi^2 F_\pi^2}\frac{2E-M_\alpha-M_\beta}{\sqrt{m_\alpha m_\beta}}g_{(\alpha)_I}(q')g_{(\beta)_I}(q), \tag{14}$$

for the E-dep model. Here, m_α (M_α) is the meson (baryon) mass of the channel α; q' (q) is the magnitude of relative momentum of the channel α (β) in the two-body CM frame; F_π is the pion decay constant; the coupling coefficients $C_{(\alpha)_I(\beta)_I}$ are summarized in Table III. As for the cutoff factors $g_{(\alpha)_I}(q')$, we employ the dipole form with the cutoff $\Lambda_{(\alpha)_I}$, $g_{(\alpha)_I}(q') = [\Lambda^2_{(\alpha)_I}/(\Lambda^2_{(\alpha)_I}+q'^2)]^2$.

TABLE III: The coupling coefficients $C_{(\alpha)_I(\beta)_I}$. Note that $C_{(\alpha)_I(\beta)_I} = C_{(\beta)_I(\alpha)_I}$.

(α,β)	Total Isospin I	$C_{(\alpha)_I(\beta)_I}$
$(\bar{K}N,\bar{K}N)$	0	6
$(\bar{K}N,\pi\Sigma)$	0	$-\sqrt{6}$
$(\pi\Sigma,\pi\Sigma)$	0	8
$(\bar{K}N,\bar{K}N)$	1	2
$(\bar{K}N,\pi\Sigma)$	1	-2
$(\bar{K}N,\pi\Lambda)$	1	$-\sqrt{6}$
$(\pi\Sigma,\pi\Sigma)$	1	4
$(\pi\Sigma,\pi\Lambda)$	1	0
$(\pi\Lambda,\pi\Lambda)$	1	0
$(\pi N,\pi N)$	1/2	4
$(\pi N,\pi N)$	3/2	-2

It is noted that except for the cutoff factors, both of the above potentials [Eqs. (13) and (14)] are derived from the so-called Weinberg-Tomozawa term [24, 25] that is the leading-order term of the effective chiral Lagrangian,

$$L_{\text{WT}} = \frac{i}{8F_\pi^2}\text{tr}(\bar{\psi}_B\gamma^\mu[[\phi,\partial_\mu\phi],\psi_B]), \tag{15}$$

with ψ_B (ϕ) being the octet baryon (pseudoscalar meson) field. From this Lagrangian, the s-wave potential is given by

$$V_{\rm WT}^{\text{s-wave}} = -\frac{C_{(\alpha)_I(\beta)_I}}{32\pi^2 F_\pi^2 \sqrt{\omega_\alpha(q')\omega_\beta(q)}} \sqrt{\frac{(E_\alpha(q')+M_\alpha)(E_\beta(q)+M_\beta)}{2E_\alpha(q')2E_\beta(q)}} \times \left[\omega_\alpha(q') + E_\alpha(q') - M_\alpha + \omega_\beta(q) + E_\beta(q) - M_\beta\right], \tag{16}$$

where $\omega_\alpha(q')$ $[E_\alpha(q')]$ is the meson [baryon] energy of the channel α. We then obtain the E-indep potential (13) from Eq. (16) by assuming $|\vec{q}\,'| \ll m_\alpha, M_\alpha$ and $|\vec{q}| \ll m_\beta, M_\beta$. On the other hand, the E-dep potential (14) are given by first replacing $\omega_\alpha(q') + E_\alpha(q')$ and $\omega_\beta(q) + E_\beta(q)$ in the brackets of Eq. (16) with the on-shell two-body scattering energy E, which is now considered to be an independent variable, and then assuming $|\vec{q}\,'| \ll m_\alpha, M_\alpha$ and $|\vec{q}| \ll m_\beta, M_\beta$. The replacement with the on-shell two-body scattering energy in deriving the E-dep potential corresponds to the so-called "on-shell factorization" [26].

As already seen in Sec. II, we take the non-relativistic kinematics for the numerical calculations. This is because of a problem inherent in the use of energy-dependent two-body potentials for the three-body calculations with the relativistic kinematics. If the relativistic kinematics are used, the total energy of the two-body subsystem can become pure imaginary for large spectator momenta [8]. However, such a difficulty does not appear as far as one uses the non-relativistic kinematics.

Parameters of the two-body potentials are the cutoffs $\Lambda_{(\alpha)_I}$. We determine the cutoffs by fitting the $I = 0$ $\pi\Sigma$ invariant mass distributions of the $K^- p \to \pi\pi\pi\Sigma$ reaction and the $\bar{K}N$ reaction cross sections. Results of the fit for the E-indep and E-dep models are presented in Fig. 3 and Fig. 4, respectively. There, the results are shown as bands because we have determined the cutoffs only up to certain ranges within which the computed cross sections are consistent with the experimental errors. The fitted values of the cutoffs are listed in Table IV.

TABLE IV: Cutoff parameters of $\bar{K}N$-πY interaction.

	$\Lambda_{(Y_K)_{I=0}}$ (MeV)	$\Lambda_{(Y_\pi)_{I=0}}$ (MeV)	$\Lambda_{(Y_K)_{I=1}}$ (MeV)	$\Lambda_{(Y_\pi=\pi\Sigma)_{I=1}}$ (MeV)	$\Lambda_{(Y_\pi=\pi\Lambda)_{I=1}}$ (MeV)
E-indep	975-1000	675-725	920	960	640
E-dep	975-1000	675-725	725	725	725

In Fig. 5, we present the resonance pole positions of the $\bar{K}N$ s-wave scattering amplitudes in the complex energy plane between the $\bar{K}N$ and $\pi\Sigma$ threshold energies. We find that

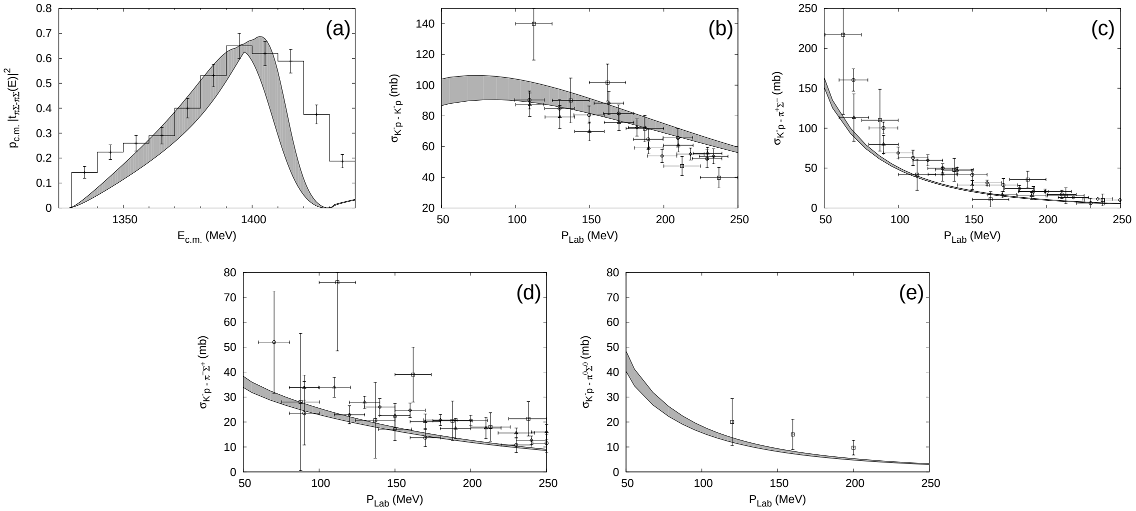

FIG. 3: Results of the fit with the E-indep model. (a) $I = 0$ $\pi\Sigma$ invariant mass distributions of $K^-p \to \pi\pi\pi\Sigma$; total cross sections of (b) $K^-p \to K^-p$, (c) $K^-p \to \pi^+\Sigma^-$, (d) $K^-p \to \pi^-\Sigma^+$, and (e) $K^-p \to \pi^0\Sigma^0$. Data are from Refs. [27–32].

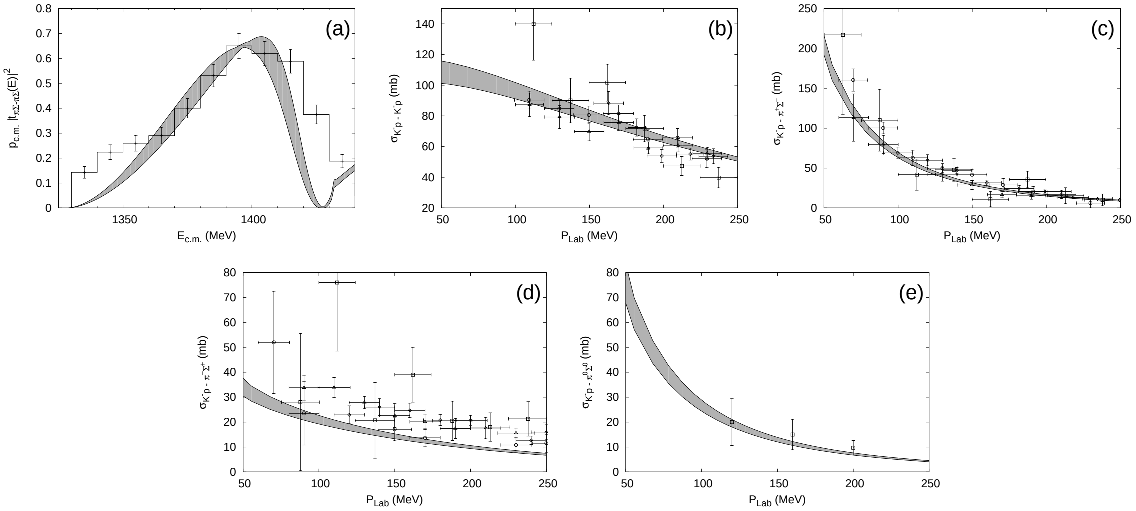

FIG. 4: Results of the fit with the E-dep model. (a) $I = 0$ $\pi\Sigma$ invariant mass distributions of $K^-p \to \pi\pi\pi\Sigma$; total cross sections of (b) $K^-p \to K^-p$, (c) $K^-p \to \pi^+\Sigma^-$, (d) $K^-p \to \pi^-\Sigma^+$, and (e) $K^-p \to \pi^0\Sigma^0$. Data are from Refs. [27–32].

the E-indep model has a single pole corresponding to $\Lambda(1405)$ in the $\bar{K}N$ physical and $\pi\Sigma$ unphysical sheet [Fig.5(a)], while the E-dep model has two poles in the same sheet [Fig.5(b)]. The analytic structure of the amplitudes in the E-dep model is similar to that obtained with the chiral unitary model [33].

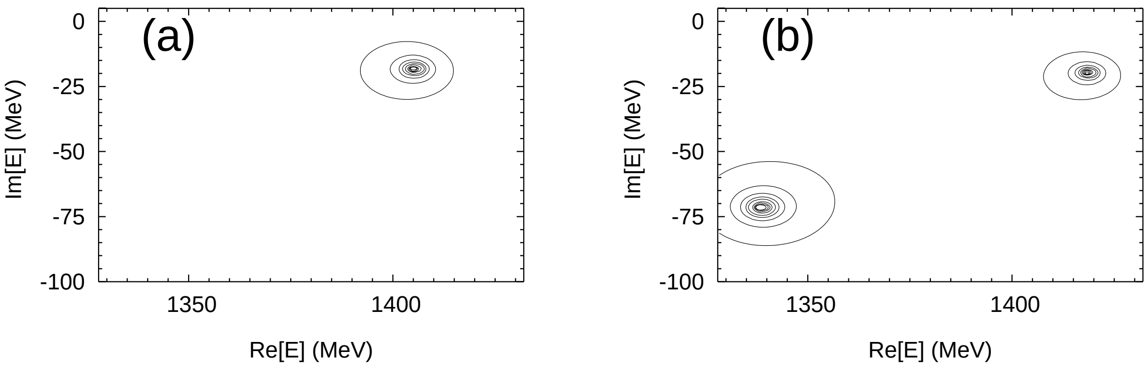

FIG. 5: The $S = -1$, $J^{\pi} = 1/2^{-}$ $\bar{K}N$ s-wave amplitude on complex energy plane in (a) the E-indep model and (b) the E-dep model. The cutoff parameters are $(\Lambda_{(Y_K)_{I=0}}, \Lambda_{(Y_\pi)_{I=0}}) = (1000, 700)$ MeV.

As for the cutoffs with $\alpha = \pi N$, we have determined them by fitting the S_{11} and S_{31} πN scattering lengths [34]. The resulting values are summarized in Table V.

TABLE V: Cutoffs of the πN interactions.

	$\Lambda_{(N^*)_{I=1/2}}$(MeV)	$\Lambda_{(N^*)_{I=3/2}}$(MeV)
E-indep model	400	400
E-dep model	400	400

B. Baryon-baryon interactions

As for the s-wave NN interactions, we take the following form [7],

$$V_{(d)_{I=1},(d)_{I=1}}(q',q) = 4\pi C_R g_R(q') g_R(q) - 4\pi C_A g_A(q') g_A(q). \tag{17}$$

Here, C_R (C_A) is the coupling strength of the repulsive (attractive) potential; The form factors $g_{R,A}(q)$ are defined by $g_{R,A}(q) = {\Lambda_{R,A}}^2/(q^2 + {\Lambda_{R,A}}^2)$ with $\Lambda_{R,A}$ being the cutoff parameters of the NN interactions. The coupling strengths $C_{R,A}$ and the cutoff parameters $\Lambda_{R,A}$ are determined by fitting the ${}^1S_0$ phase shifts [35] (see Fig. 6 for the result of the fit). The resulting values of the parameters are summarized in Table VI.

As for the s-wave YN interactions, we follow the form given in Ref. [36],

$$V_{(\alpha)_I,(\beta)_I}(q',q) = -4\pi \frac{C_{(\alpha)_I(\beta)_I}}{2\pi^2} (\mu_\alpha \mu_\beta \Lambda_{(\alpha)_I} \Lambda_{(\beta)_I})^{-1/2} g_{(\alpha)_I}(q') g_{(\beta)_I}(q). \tag{18}$$

TABLE VI: Parameters of NN interaction.

Λ_R(MeV)	Λ_A(MeV)	C_R(MeV fm^3)	C_A(MeV fm^3)
1215	352	5.05	5.84

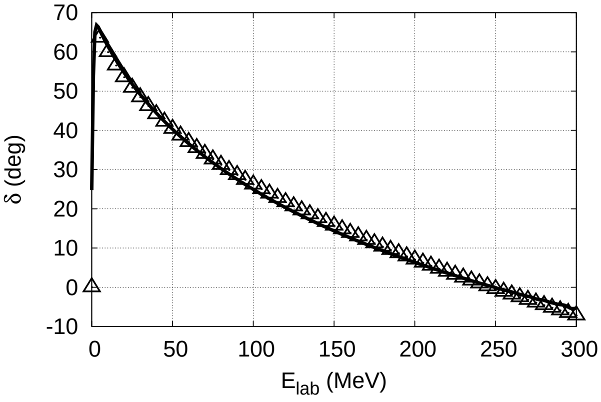

FIG. 6: Phase shifts of NN scattering for the $^1S_0$ state. The solid line shows the phase shift with our model, and triangles show the phase shifts with the model of Ref. [35].

Here, $C_{(\alpha)_I(\beta)_I}$ are the coupling constants given by $C_{(\Sigma N)_I(\Sigma N)_I} = 0.83$, $C_{(\Sigma N)_I(\Lambda N)_I} = 0.56$, and $C_{(\Lambda N)_I(\Lambda N)_I} = 0.49$ for $I = 1/2$, and $C_{(\Sigma N)_I(\Sigma N)_I} = -0.29$ for $I = 3/2$; μ_α is the reduced mass for the YN system; the form factor $g_{(\alpha)_I}(q)$ is defined by $g_{(\alpha)_I}(q) = \Lambda^2_{(\alpha)_I}/(q^2 + \Lambda^2_{(\alpha)_I})$; the cutoff parameters $\Lambda_{(\alpha)_I}$ are given by $\Lambda_{(\Sigma N)_I} = 251$ MeV and $\Lambda_{(\Lambda N)_I} = 262$ MeV.

IV. RESULTS AND DISCUSSION

A. Quasi-two-body scatterings

Now we present the partial-wave quasi-two-body amplitudes at the real scattering energies W, $X_{(\alpha)_I i,(\beta)_{I'} j}(p_i, p_j, W)$, which are obtained by solving the coupled-channel AGS equation (6) and using the point method explained in Appendix. In Fig.7, we present the absolute square of the amplitudes, $|X_{(Y_K)_{I=0}N,(Y_K)_{I=0}N}(p_i, p_j, W)|^2$, whose initial- and final-state isobars are (Y_K) with the isospin $I = 0$. Here we plot the results of the E-indep (E-dep) model as solid (dashed) curves. Also, we plot the amplitudes with two different cases of the off-shell momentum for each model, with $p_i = p_j = 150$ MeV for thick curves and with

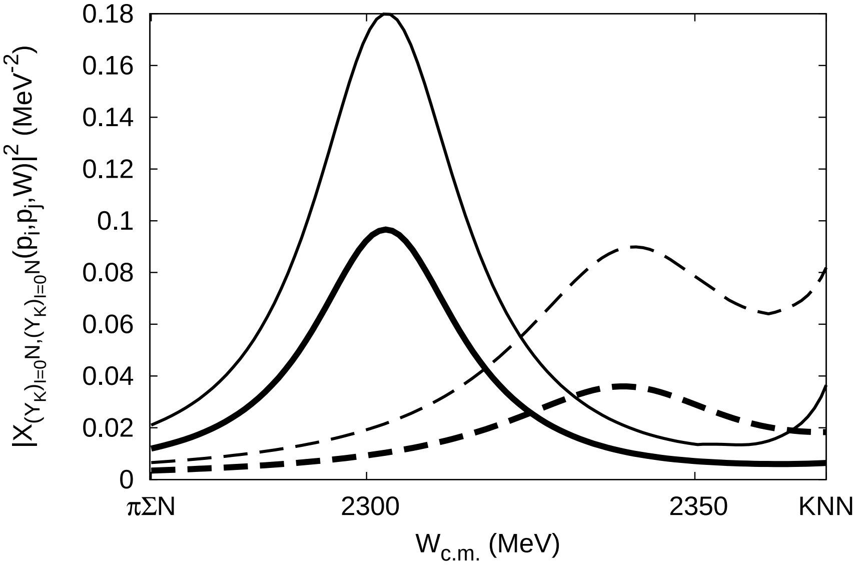

FIG. 7: W dependence of $|X_{(Y_K)_{I=0}N,(Y_K)_{I=0}N}(p_i, p_j, W)|^2$. Each curve is: (solid curves) the E-indep model; (dashed curves) the E-dep model; (thick curves) $p_i = p_j = 150$ MeV; (thin curves) $p_i = p_j = 100$ MeV. The cutoff parameters are taken to be $(\Lambda_{(Y_K)_{I=0}}, \Lambda_{(Y_\pi)_{I=0}}) = (1000, 700)$ MeV.

$p_i = p_j = 100$ MeV for thin curves, to examine the momentum dependence of the amplitudes. We find both models have a bump between the $\bar{K}NN$ and $\pi\Sigma N$ threshold energies: $W \sim 2305$ MeV for the E-indep model and $W \sim 2340$ MeV for the E-dep model, both of which are close to the resonance pole masses M_R with $-\mathrm{Im}(M_R) \sim 20$ MeV (see Table I). Furthermore, the positions of the bumps are independent of the momentum, and thus we can conclude that these bumps are actually produced by the strange dibaryon resonances. On the other hand, in the E-dep model, another strange dibaryon with $-\mathrm{Im}(M_R) \sim 100$ MeV barely affects the amplitude on the physical real energy axis. This is consistent with the fact that normally resonances with large widths cannot produce a sharp peak in the absolute square of the amplitudes or cross sections. In Fig. 8, we show the W dependence of the amplitudes with different final states. We observe that the bumps due to the strange dibaryon resonances appear at almost the same W regardless of the final quasi-two-body states, as it should be.

Next we present the contributions of each one-particle-exchange mechanism Z to the amplitude $|X_{(Y_K)_{I=0}N,(Y_K)_{I=0}N}(p_i, p_j, W)|^2$ with $p_i = p_j = 100$ MeV (Fig. 9). Here the solid curve in Fig. 9(a) [Fig. 9(b)] is same as the thin-solid (thin-dashed) curve in Fig. 7. If the baryon-

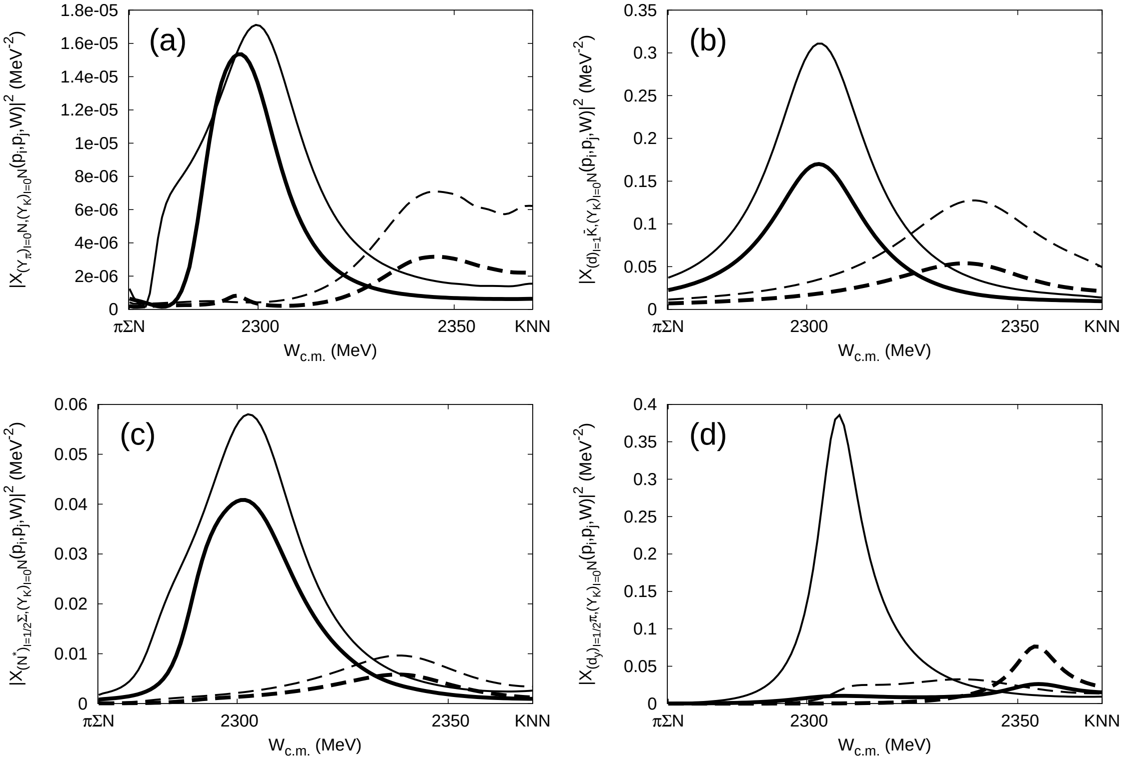

FIG. 8: W dependence of $|X_{(\alpha)_I i, Y_k(I=0)N}(p_i, p_j, W)|^2$. (a) $(\alpha)_I = (Y_\pi)_{I=0}$ and $i = N$, (b) $(\alpha)_I = (d)_{I=1}$(repulsive) and $i = \bar{K}$, (c) $(\alpha)_I = (N^*)_{I=1/2}$ and $i = \Sigma$, and (d) $(\alpha)_I = (d_y)_{I=1/2}$ and $i = \pi$. The meaning of each curve and the cutoff parameters are taken to be the same as in Fig. 7.

exchange (meson-exchange) Z-potentials are switched off in the rescattering processes, then the solid curves in Fig. 9 are turned into the dashed (dotted) curves. Contributions of the meson-exchange processes seem to be crucial for producing the similar bump structure to the full amplitudes, while those of the baryon-exchange processes do not. However, we also observe that rescattering effects including both the meson- and baryon-exchange processes, which are required by the three-body unitarity, amplify the magnitude of the scattering amplitudes significantly, indicating the importance of maintaining the three-body unitarity exactly in searching for the evidence of the strange dibaryon resonances.

B. Transition probability for the break-up $(Y_K)_{I=0} + N \to \pi + \Sigma + N$ reaction.

Finally, we investigate the energy dependence of the transition probability, $w(p_N, W)$ defined in Eq. (12), for the $(Y_K)_{I=0} + N \to \pi + \Sigma + N$ break-up reaction. In Fig. 10, we

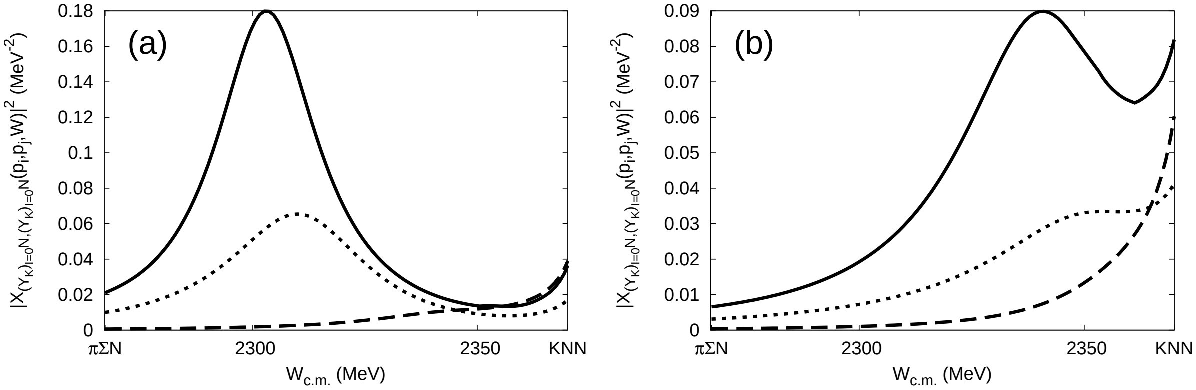

FIG. 9: Contributions of one-particle-exchange processes to $|X_{(Y_K)_{I=0}N,(Y_K)_{I=0}N}(p_i,p_j,W)|^2$. The figures are for (a) the E-indep model and (b) the E-dep model. Each curve is: (solid curves) full results; (dashed curves) baryon-exchange processes only; (dotted curves) meson-exchange processes only. The momentum [cutoff parameters] are fixed as $p_i = p_j = 100$ MeV $[(\Lambda_{(Y_K)_{I=0}}, \Lambda_{(Y_\pi)_{I=0}}) = (1000, 700)$ MeV].

present $w(p_N, W)$ for $p_N = 100$ MeV and $p_N = 150$ MeV using the same values of parameters as used in Fig. 7. We again find that the position of the bumps in $w(p_N, W)$ are independent of the momentum p_N of the initial $(Y_K)N$ channel, implying that the bumps originate from the strange dibaryon resonances. The E-indep and E-dep models are found to produce quite different energy dependence on the transition probabilities; those differences would be large enough to be detected by experiments. Because this difference is closely related to the different nature of $\Lambda(1405)$ between the two models as shown in Fig. 5, the strange dibaryon production reactions would also provide critical information on the dynamical origin of $\Lambda(1405)$.

Next we examine the cutoff parameter dependence on the transition probability $w(p_N, W)$ (Fig. 11). The bands are given by varying the values of $\Lambda_{(Y_K)_{I=0}}$ and $\Lambda_{(Y_\pi)_{I=0}}$ within the allowed range listed in Table IV. We see that the signal of the strange dibaryon resonances remains to be observed in the transition probability within the allowed range of $\Lambda_{(Y_K)_{I=0}}$ and $\Lambda_{(Y_\pi)_{I=0}}$.

Finally, we examine the contribution of each reaction process to the transition probability (Fig. 12). As can be seen in Eq. (11), the reaction processes consist of the quasi two-body processes characterized by the amplitudes $X_{(Y_K)_I N,(Y_K)_{I=0}N}$, $X_{(Y_\pi)_I N,(Y_K)_{I=0}N}$,

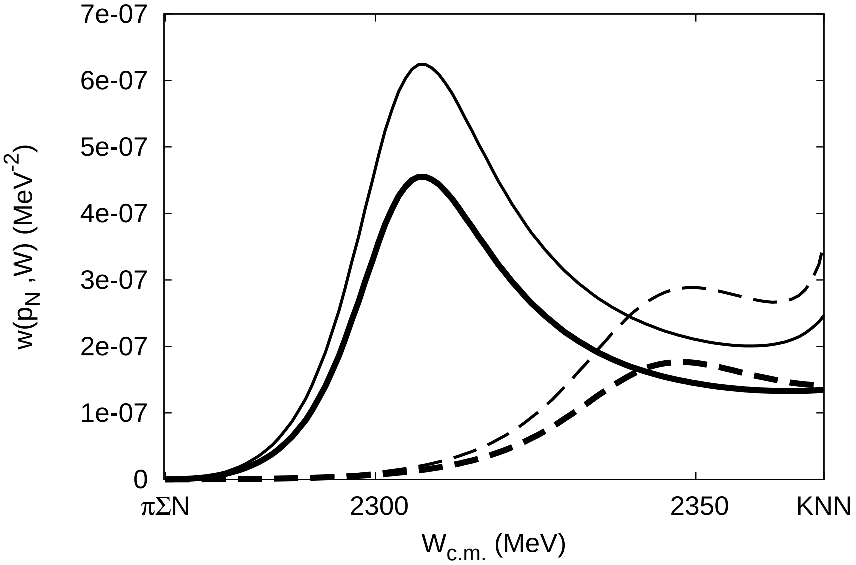

FIG. 10: Total transition probability $w(p_N, W)$ for $(Y_K)_{I=0} + N \to \pi + \Sigma + N$. The meaning of each curve and the cutoff parameters are taken to be same as in Fig. 7.

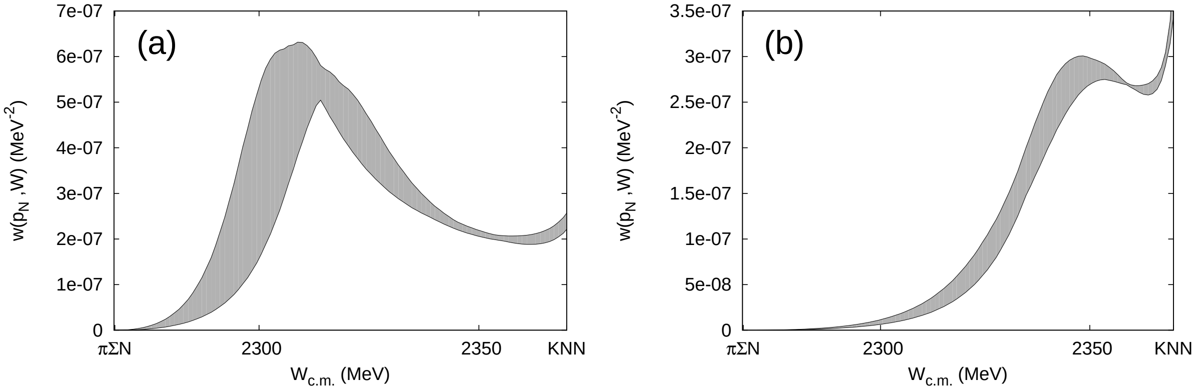

FIG. 11: Cutoff dependence on the transition probability for the $(Y_K)_{I=0} + N \to \pi + \Sigma + N$ reaction. Panel (a): the E-indep model; Panel (b) the E-dep model. The bands of transition probability are produced by varying values of $\Lambda_{(Y_K)_{I=0}}$ and $\Lambda_{(Y_\pi)_{I=0}}$ in the allowed range listed in Table IV. The initial nucleon momentum is set to $p_N = 100$ MeV.

$X_{(N^*)_I\Sigma,(Y_K)_{I=0}N}$, and $X_{(d_y)_I\pi,(Y_K)_{I=0}N}$. We find that the $X_{(Y_K)_{I=0}N,(Y_K)_{I=0}N}$ process has dominant contribution about 85% to the transition probability, while others have rather small contributions: about 5% is from $X_{(d_y)_I\pi,(Y_K)_{I=0}N}$, and less than 1% is from $X_{(Y_\pi)_IN,(Y_K)_{I=0}N}$ and $X_{(N^*)_I\Sigma,(Y_K)_{I=0}N}$.

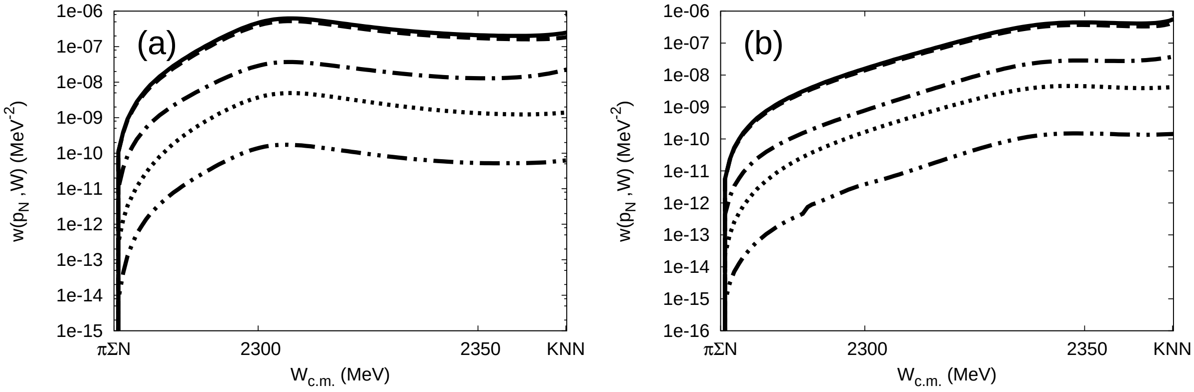

FIG. 12: Contribution of each quasi-two-body process to the $(Y_K)_{I=0}+N \rightarrow \pi+\Sigma+N$ transition probability. The figures are for (a) the E-indep model and (b) the E-dep model. Each curve is: (solid curve) Full results; (dashed curve) $X_{(Y_K)_I N,(Y_K)_{I=0}N}$ process only; (dashed-two-dotted curve) $X_{(Y_\pi)_I N,(Y_K)_{I=0}N}$ process only; (dotted curve) $X_{(N^*)_I \Sigma,(Y_K)_{I=0}N}$ process only; (dashed-dotted curve) $X_{(d_y)_I \pi,(Y_K)_{I=0}N}$ process only. The cutoff parameters $\Lambda_{(Y_K)_{I=0}}$ and $\Lambda_{(Y_\pi)_{I=0}}$ are taken to be 1000 MeV and 700 MeV, respectively, and the initial nucleon momentum is set to $p_N = 100$ MeV.

V. SUMMARY

Within the framework of the coupled-channel AGS equations, we have examined how the signature of the strange dibaryon resonances in the three-body $\bar{K}NN$-πYN system shows up in the scattering amplitudes and transition probabilities on the physical real energy axis. The logarithmic singularities appearing in solving the AGS equations for the real scattering energies have been successfully handled by making use of the point method. Two different kinds of models, the E-indep and E-dep models, have been considered for the two-body $\bar{K}N$-$\pi\Sigma$ subsystem to investigate whether the strange-dibaryon production reactions can be used for disentangling the nature of the two-body $\bar{K}N$-$\pi\Sigma$ system with $\Lambda(1405)$.

We have found that within our model, a clear bump produced by strange dibaryon resonances appear in the quasi-two-body scattering amplitudes $X_{(\alpha)_I i,(Y_K)_{I=0}N}(W)$ and the $(Y_K)_{I=0} + N \rightarrow \pi + \Sigma + N$ transition probabilities in the energy region between the $\bar{K}NN$ and $\pi\Sigma N$ thresholds, which strongly suggests that the clear signals of strange dibaryon resonances should be detected by measuring of $\pi\Sigma N$ invariant mass distributions at the relevant energies. We have also found that the E-indep and E-dep models produce quite different energy dependence on $X_{(\alpha)_I i,(Y_K)_{I=0}N}(W)$ and $(Y_K)_{I=0} + N \rightarrow \pi + \Sigma + N$ transition probabilities; those differences would be large enough to be detected by experiments. Within our framework, this difference originates from the different nature of $\Lambda(1405)$ between the two models as shown in Fig. 5, and thus the strange dibaryon production reactions would also be helpful to reveal the dynamical origin of $\Lambda(1405)$.

It is for the first time that the break-up $(Y_K)_{I=0} + N \to \pi + \Sigma + N$ transition probabilities are computed within the fully coupled-channel AGS equations. As a next step, we will further account for initial state interactions and develop a technique to make practical calculations of "actual" cross sections of kaon- and photon-induced strange dibaryon production reactions shown in Fig. 1, which will be measured at experimental facilities such as J-PARC and SPring-8. This will be discussed elsewhere.

Acknowledgments

The simulation has been done on a supercomputer (NEC SX8R) at Research Center for Nuclear Physics, Osaka University. This work is partly supported by Yamada Science Foundation. YI and HK acknowledge the support by the HPCI Strategic Program (Field 5 "The Origin of Matter and the Universe") of Ministry of Education, Culture, Sports, Science and Technology (MEXT) of Japan. TS is supported by JSPS KAKENHI (Grant Number 24540273).

Appendix A: Brief description of the point method

The s-wave projection of the particle-exchange potential, $Z_{(\alpha)_I i,(\beta)_{I'} j}(p_i, p_j, W)$ [Eq. (4)], contains the following logarithm,

$$\ln\left[\frac{W - M - \frac{p_i^2}{2m_i} - \frac{p_j^2}{2m_j} - \frac{p_i^2+p_j^2-2p_ip_j}{2m_k}}{W - M - \frac{p_i^2}{2m_i} - \frac{p_j^2}{2m_j} - \frac{p_i^2+p_j^2+2p_ip_j}{2m_k}}\right] \quad . \tag{A1}$$

For real W with $W > M$, this logarithm becomes singular at momentum (p_i, p_j) satisfying

$$W - M - \frac{p_i^2}{2m_i} - \frac{p_j^2}{2m_j} - \frac{p_i^2 + p_j^2 \pm 2p_ip_j}{2m_k} = 0 \quad . \tag{A2}$$

The singularities appear as a "moon-shape" in the p_i-p_j plane as illustrated in Fig. 13.

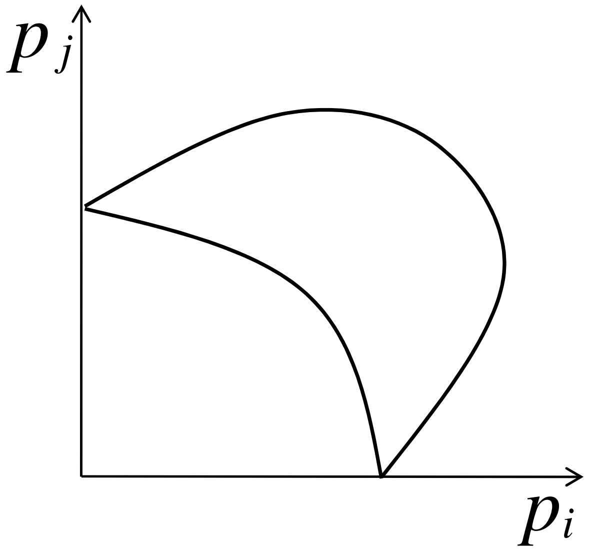

FIG. 13: The moon-shape singularities. Solid curve shows the momentum (p_i, p_j) where $Z_{(\alpha)_I i,(\beta)_{I'} j}(p_i, p_j, W)$ has logarithmic singularity.

As a practical technique to handle the moon-shape singularities in solving the scattering equations (6), we have employed the point method, which is proposed by Schlessinger [22] and developed by Kamada *et al.* [23]. We briefly explain the method in the following.

The point method is an extrapolation technique of functions. With this technique, one can evaluate the value of a function $X(W)$ of real W from $X(W+i\epsilon_i)$, where ϵ_i $(\epsilon = 1, 2, ...)$ is a series of positive finites that converges to zero, using the following formulas,

$$X(W) = \lim_{\epsilon\to 0} \frac{X(W+i\epsilon_1)}{1+\frac{a_1(\epsilon-\epsilon_1)}{1+\cdots}} = \lim_{\epsilon\to 0} \frac{X(W+i\epsilon_1)}{1+} \frac{a_1(\epsilon-\epsilon_1)}{1+} \frac{a_2(\epsilon-\epsilon_2)}{1+} \cdots \quad , \tag{A3}$$

with

$$a_l = \frac{1}{\epsilon_l - \epsilon_{l+1}} \left(1 + \frac{a_{l-1}(\epsilon_{l+l} - \epsilon_{l-1})}{1+} \frac{a_{l-2}(\epsilon_{l+1} - \epsilon_{l-1})}{1+} \cdots \frac{a_1(\epsilon_{l+1} - \epsilon_1)}{1 - [X(W+i\epsilon_1)/X(W+i\epsilon_{l+1})]} \right) \tag{A4}$$

To illustrate how we get scattering amplitudes $X_{(\alpha)_I i,(\beta)_{I'} j}(p_i, p_j, W)$ for real W, we apply the formulas above to the Amado model [20], a simple model for three-boson scatterings. The AGS equations for the s-wave scattering of a boson b and a two-b bound-state d, $bd \to bd$, are given by

$$X(p', p_0, W) = 2Z(p', p, W) + 2 \int p^2 dp Z(p', p, W) \tau(p, W) X(p, p_0, W). \tag{A5}$$

In the bd CM system, the driving term $Z(p', p, W)$ and the two-body propagator $\tau(p, W)$ are expressed as

$$Z(p', p, W) = \frac{1}{2}\int_{-1}^{1} dx \frac{g_0}{(|\vec{p'} + \frac{1}{2}\vec{p}|^2 + \beta^2)} \frac{g_0}{(|\vec{p} + \frac{1}{2}\vec{p'}|^2 + \beta^2)} \times \frac{1}{W' - \frac{p^2}{2m} - \frac{p'^2}{2m} - \frac{(\vec{p}+\vec{p'})^2}{2m} + i\epsilon}, \tag{A6}$$

$$\begin{aligned} \tau^{-1}(p, W) &= [E_2(p, W') + B + i\epsilon] \\ &= \left[1 - (E_2(p, W') + B + i\epsilon) \int k^2 dk \frac{g^2(k)}{\left(B + \frac{k^2}{m}\right)^2 \left(E_2(p, W') - \frac{k^2}{m} + i\epsilon\right)}\right]. \end{aligned} \tag{A7}$$

Here, $g(q) = g_0/(q^2 + \beta^2)$ is the form factor for $d \to bb$, which is normalized as $\int k^2 dk g^2(k)/(B + \frac{k^2}{m})^2 = 1$; B is binding energy of d, and $E_2(p, W) = W - 3p^2/(4m)$ is two-body scattering energy. We solve these AGS equations by setting $\hbar = 2m = 1$, $B = 1.5$, $\beta = 5$, and $W' = 1$.

If one tries to solve Eq. (A5) for a real W, the momentum integral path crosses the singularities of the Z potential and thus the resulting amplitude $X(p', p_0, W)$ does not converge. On the other hand, one can have convergent solutions of Eq. (A5) without any problems for complex energies $W + i\epsilon_l$ with positive finites ϵ_l. Therefore, we first compute the amplitude X for several complex energies, and then make an extrapolation to $X(W)$ using Eqs. (A3) and (A4). For practical computations, we use five ϵ_l's,

$$\epsilon_l = 0.05 \times l \qquad (l = 1, 2, \ldots, 5). \tag{A8}$$

In Fig. 14, we show the p dependence of $X(p, p_0, W)$ for $W = 1$ and $p_0 = \sqrt{4m(W + B)/3}$. The solid (dashed) curve represents the real (imaginary) part of the amplitude $X(p, p_0, W)$ extrapolated using the point method. In the same figure, we also present the amplitude obtained by the spline interpolation method [37] as a comparison.

The scattering amplitude $X(W)$ for the $\bar{K}NN$-πYN system studied in this work is extrapolated from the amplitude $X(W + i\epsilon_l)$ at $\epsilon_l = 10 \times l$ (MeV) for $l = 1, 2, \ldots, 5$, using Eqs. (A3) and (A4).

---

[1] Y. Akaishi and T. Yamazaki, Phys. Rev. C **65**, 044005 (2002).

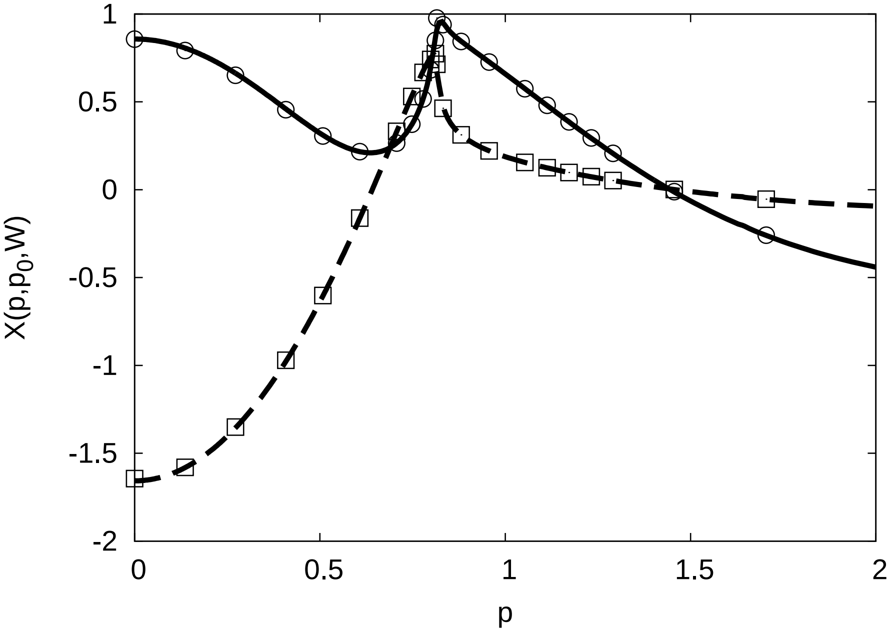

FIG. 14: The amplitude $X(p, p_0, W)$ of the Amado model at $W = 1$ and the on-shell momentum $p_0 = \sqrt{4m(W + B)/3}$. Solid and dashed curves are the real and imaginary parts of the amplitude $X(p, p_0, W)$, respectively, extrapolated by the point method [22, 23]. Circles and squares are the real and imaginary parts of the amplitude $X(p, p_0, W)$ by the spline interpolation method [37].

[2] T. Yamazaki and Y. Akaishi, Phys. Lett. B **535**, 70 (2002);
T. Yamazaki and Y. Akaishi, Phys. Rev. C **76**, 045201 (2007) [arXiv:0709.0630 [nucl-th]].

[3] A. Dote, T. Hyodo and W. Weise, Nucl. Phys. A **804**, 197 (2008) [arXiv:0802.0238 [nucl-th]];
A. Dote, T. Hyodo and W. Weise, Phys. Rev. C **79**, 014003 (2009) [arXiv:0806.4917 [nucl-th]].

[4] S. Wycech and A. M. Green, Phys. Rev. C **79**, 014001 (2009) [arXiv:0808.3329 [nucl-th]].

[5] N. Barnea, A. Gal and E. Z. Liverts, Phys. Lett. B **712**, 132 (2012) [arXiv:1203.5234 [nucl-th]].

[6] N. V. Shevchenko, A. Gal and J. Mares, Phys. Rev. Lett. **98**, 082301 (2007) [arXiv:nucl-th/0610022];
N. V. Shevchenko, A. Gal, J. Mares and J. Revai, Phys. Rev. C **76**, 044004 (2007) [arXiv:0706.4393 [nucl-th]].

[7] Y. Ikeda and T. Sato, Phys. Rev. C **76**, 035203 (2007) [arXiv:0704.1978 [nucl-th]];
Y. Ikeda and T. Sato, Phys. Rev. C **79**, 035201 (2009) [arXiv:0809.1285 [nucl-th]].

[8] Y. Ikeda, H. Kamano and T. Sato, Prog. Theor. Phys. **124**, 533 (2010) [arXiv:1004.4877 [nucl-th]].

[9] T. Hyodo and W. Weise, Phys. Rev. C **77**, 035204 (2008) [arXiv:0712.1613 [nucl-th]].

[10] M. Agnello *et al.* [FINUDA Collaboration], Phys. Rev. Lett. **94**, 212303 (2005).

[11] G. Bendiscioli, A. Fontana, L. Lavezzi, A. Panzarasa, A. Rotondi and T. Bressani, Nucl. Phys. A **789**, 222 (2007).

[12] T. Yamazaki *et al.* [DISTO Collaboration], arXiv:0810.5182 [nucl-ex];
T. Yamazaki, M. Maggiora, P. Kienle, K. Suzuki, A. Amoroso, M. Alexeev, F. Balestra and Y. Bedfer *et al.*, Phys. Rev. Lett. **104**, 132502 (2010) [arXiv:1002.3526 [nucl-ex]].

[13] J. D. Parker [LEPS Collaboration], Mod. Phys. Lett. A **23**, 2544 (2008).

[14] K. Suzuki *et al.* [FOPI Collaboration], Prog. Theor. Phys. Suppl. **186**, 351 (2010).

[15] M. Iwasaki *et al.*, J-PARC E15 proposal.
http://j-parc.jp/researcher/Hadron/en/pac_0606/pdf/p15-Iwasaki.pdf

[16] T. Nagae *et al.*, J-PARC E27 proposal.
http://www.j-parc.jp/researcher/Hadron/en/pac_0907/pdf/Nagae.pdf

[17] J. Zmeskal [AMADEUS Collaboration], Int. J. Mod. Phys. A **26**, 414 (2011).

[18] T. Koike and T. Harada, Phys. Rev. C **80**, 055208 (2009) [arXiv:0906.3659 [nucl-th]].

[19] J. Yamagata-Sekihara, D. Jido, H. Nagahiro and S. Hirenzaki, Phys. Rev. C **80**, 045204 (2009) [arXiv:0812.4359 [nucl-th]].

[20] R. D. Amado, Phys. Rev. **132**, 485 (1963).

[21] E. O. Alt, P. Grassberger and W. Sandhas, Nucl. Phys. B **2**, 167 (1967).

[22] L. Schlessiner, Phys. Rev. **167**, 1411 (1968).

[23] H. Kamada, Y. Koike and W. Gloeckle, Prog. Theor. Phys. **109**, 869 (2003) [arXiv:nucl-th/0301018].

[24] S. Weinberg, Phys. Rev. Lett. **17**, 616 (1966).

[25] Y. Tomozawa, Nuovo Cim. A **46**, 707 (1966).

[26] E. Oset and A. Ramos, Nucl. Phys. A **635**, 99 (1998) [nucl-th/9711022].

[27] R. J. Hemingway, Nucl. Phys. B **253**, 742 (1985).

[28] W. E. Humphrey and R. R. Ross, Phys. Rev. **127**, 1305 (1962).

[29] M. Sakitt, T. B. Day, R. G. Glasser, N. Seeman, J. H. Friedman, W. E. Humphrey and R. R. Ross, Phys. Rev. **139**, B719 (1965).

[30] J. K. Kim, Phys. Rev. Lett. **14**, 29 (1965).

[31] W. Kittel, G. Otter and I. Wacek, Phys. Lett. **21**, 349 (1966).

[32] D. Evans, J. V. Major, E. Rondio, J. A. Zakrzewski, J. E. Conboy, D. J. Miller and T. Tymieniecka, J. Phys. G **9**, 885 (1983).

[33] D. Jido, J. A. Oller, E. Oset, A. Ramos and U. G. Meissner, Nucl. Phys. A **725**, 181 (2003) [arXiv:nucl-th/0303062].

[34] H. C. Schroder *et al.*, Phys. Lett. B **469**, 25 (1999).

[35] V. G. J. Stoks, R. A. M. Klomp, C. P. F. Terheggen and J. J. de Swart, Phys. Rev. C **49**, 2950 (1994) [arXiv:nucl-th/9406039].

[36] M. Torres, R. H. Dalitz and A. Deloff, Phys. Lett. B **174**, 213 (1986).

[37] A. Matsuyama, T. Sato and T. S. Lee, Phys. Rept. **439**, 193 (2007) [arXiv:nucl-th/0608051].